

OPTICS, LASERS, AND MOLECULES: A STUDY OF RAMAN SPECTROSCOPY

Stephen Carr, Mojin Chen, Brian Delancy, Jason Elefant, Alice Huang,
Nathaniel May, Avinash Moondra, John Nappo, Nicholas Paggi,
Samuel Rosin, Marlee Silverstein, Daniel Zhang

Advisor: Dr. Robert Murawski
Assistant: Aaron Loether

ABSTRACT

Raman spectroscopy is a technique that can be used to examine the rotational and vibrational states of a molecule, as well as the number, strength, and identity of chemical bonds. It is a process in which photons interact with a sample to produce scattered radiation of varying wavelengths. Spectroscopy has been widely used across various fields to identify water and air pollutants, in addition to proving useful with a multitude of other applications. In this study of optics, lasers, and molecules, Raman spectroscopy was used to analyze different samples of water to test for impurities and the presence of foreign molecules. Samples tested included alcohols, water, and fertilizer. From the data collected, the accuracy of the setups could be confirmed by comparing alcohol spectra to accepted Raman readings and identify additional chemical components in fountain water and Glaceau SmartWater, a brand of bottled water. In addition, samples of various concentrations of fertilizer were analyzed to verify major chemical components as well as relate the concentration and intensity of the Raman signal.

INTRODUCTION/BACKGROUND

Optics

Optics is the study of light and its interactions with matter. Light, or electromagnetic radiation, exhibits both wave and particle properties, and this wave-particle duality is responsible for many of light's behaviors. The wave-like properties of this electromagnetic radiation are exhibited in behaviors such as reflection (return of a wave from the original medium off an interface back into the original medium), refraction (bending of a wave as it passes from one index of refraction to another) and diffraction (bending of waves as it passes through openings). The particle properties are exhibited in the idea of light quantization, which states that light is composed of individual particles, called photons¹.

Light has several wave properties that are integral to its interaction with matter, including wavelength and frequency. The wavelength of light is the distance between corresponding points on consecutive crests. The frequency of light is the number of complete cycles that pass through a given point each second. These two quantities relate to the speed of light with the equation

$$c = f\lambda \quad (1)$$

where c is the speed of light, f is the frequency, and λ is the wavelength. Along with these wave properties, the equation for the energy of light demonstrates its particle nature. Discovered by Max Planck, the equation

$$E = hf \quad (2)$$

indicates that the energy of a photon of light with particular frequency is equal to the frequency multiplied by Planck's constant $h = 6.626 \times 10^{-34} \text{ J}\cdot\text{s}$.

Another major topic of study in optics is that of lenses. Lenses are optical devices with particular curvatures that are used to refract light. They are usually made of glass. Converging lenses are lenses that bend rays of light towards each other². If a light source originates from the focus of a converging lens, all beams of light will emerge from the lens parallel to the principal axis. Conversely, all beams of light that pass parallel to the principal axis of a converging lens are refracted such that they pass through the focus (Fig. 1). However, lenses with spherical surfaces sometimes encounter spherical aberration, which occurs when rays parallel to the optic axis are unable to converge to the same point³. To completely eliminate spherical aberrations, a perfect paraboloid shape is needed. The curvature of the lens determines the focal length, and all light beams that pass through the center of the lens will emerge from the other side unaltered.

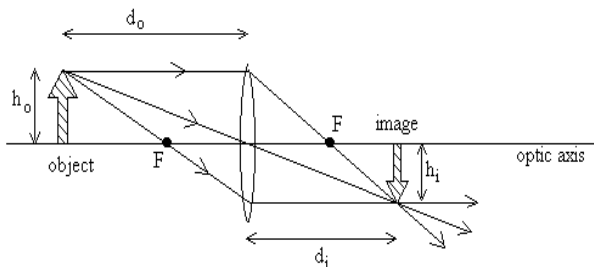


Figure 1. Converging Lens⁴. An object (height h_o) is focused through a convex converging lens. Three specific light rays are emitted from the object, and it is placed before the focal point F , where its image appears smaller and inverted.

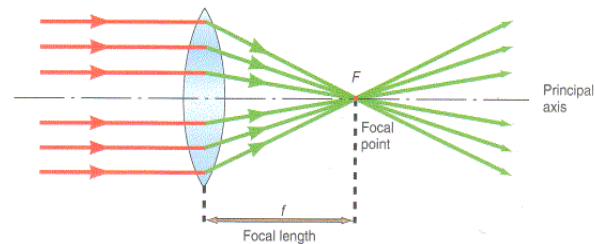


Figure 2. Convergence of Parallel Beams⁵. If a lens is placed in the path of parallel beams, the light will focus to a point. The distance between the lens and the point is called the focal length.

Finally, because of the refraction of light and Snell's Law, which pertains to indices of refraction, if the angle at which light strikes a particular interface is too high, no light will pass through and total internal reflection will occur⁶. This principle is the basis for fiber optic cables (Fig. 3), much like the ones used in our experiment, and has revolutionized the information industry.

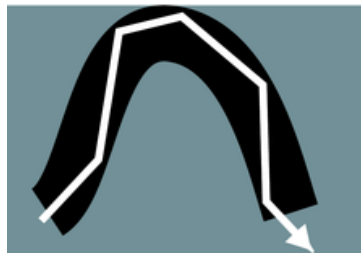


Figure 3. Fiber Optic Cable⁷.

According to Snell's Law, light is reflected along the cable's inner surface.

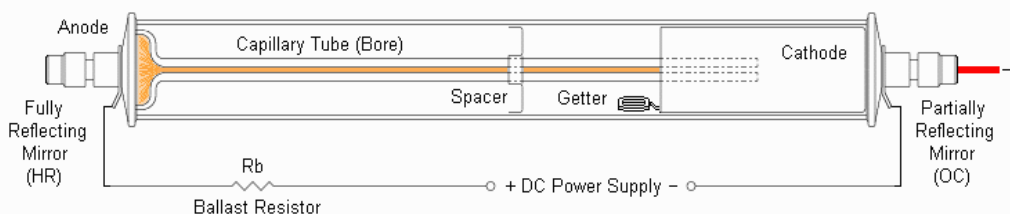
Lasers

Light Amplification by Stimulated Emission of Radiation (LASER) allows for high accuracy measurements pertaining to electromagnetic radiation by providing a highly concentrated beam of photons. Lasers emit monochromatic light that is completely in phase, and is thus much better suited for use in electromagnetic analyses than other light sources. Moreover,

laser beams can be easily manipulated by the previously described lenses and other optical devices.

Helium-Neon laser

A helium-neon (HeNe) gas laser (Fig. 4) was the first type of laser used in this study. Each laser that we used consisted of an optical cavity containing a gas tube with a mirror at each end. The gas tube, true to the name of the laser, held a gain medium consisting of helium and neon gas. Once a direct current power source is passed through the medium, a plasma state is created by exciting electrons in the helium atoms. These electrons rise to a metastable state and increase the rate of collision between helium and neon atoms, resulting in a transfer of energy that excites the electrons in the neon atoms⁸. As photons travel back and forth between the two mirrors, more photons are emitted through stimulated emission and spontaneous emission. Stimulated emission occurs when an electron, agitated by a photon of the same wavelength, drops to a lower energy level, thus emitting a new photon. Spontaneous emission occurs when an excited electron drops to a lower energy level without the assistance of a photon. The photons emitted by the neon electrons are approximately 632.8 nm in wavelength. An output coupler mirror at one end of the optical cavity permits about 1% of the photons to pass through, forming the red beam that can be seen from outside the laser.



Typical HeNe Laser Tube Structure and Connections

Figure 4. HeNe Laser⁹. A diagram of Helium-Neon Laser components.

Argon ion laser

The second laser used in this study was an argon ion laser. The argon ion laser is the same as the helium-neon laser at both a fundamental and operational level, except it uses argon ions as the gain medium rather than helium and neon gas. In an argon ion laser, a neutral argon atom gains energy after colliding with two electrons¹⁰. Later, the electrons in the excited argon ion fall to a lower energy level, either spontaneously or when stimulated by photons, thereby releasing more photons. The argon ion laser used in this experiment produced a teal-blue beam with a wavelength of 488 nanometers.

Spectroscopy

As one of the main disciplines for analytical chemistry, spectroscopy governs the examination of properties and classification on the molecular level. In the simplest form, spectroscopy is the collection and interpretation of electromagnetic radiation emitted or absorbed by excited matter. The first recorded spectroscopic experiment was performed by Sir Isaac Newton in 1666. Newton used a prism to disperse sunlight into the full visible spectrum¹¹ (Fig.

5). The basic equipment for a spectrometer was defined by this first recorded test, which consisted of an aperture to isolate a beam of light, a lens to focus the beam, a prism to diffract the focused beam, and finally a screen to allow for the observation of the emission spectrum. Although this experiment set a precedent for the procedure and setup of a spectrometer, the full impact of spectral analysis was unknown to Newton. Scientists who later built upon this first trial began to record the presence of spectral lines. In 1814, Fraunhofer discovered dark lines in greatly dispersed sun light spectra, which were later dubbed Fraunhofer's lines¹¹. Fraunhofer's lines were soon applied to astrophysics, specifically to the study of stars, but the application of spectroscopy in chemistry and other branches of physics were still undeveloped.

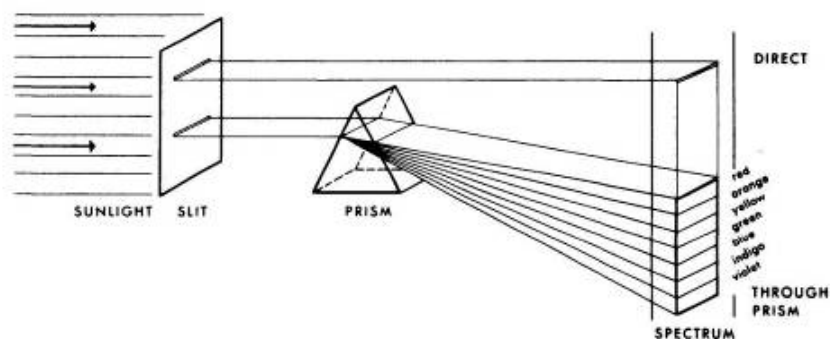


Figure 5. Newton's Spectrometer¹². A basic spectrometer consisting of a slit and a prism used to disperse white light into the entire visible spectrum.

In 1859, spectroscopy was finally linked to chemical analysis by a number of landmark experiments by German physicist Gustav Kirchhoff¹¹. Kirchhoff proved that each element, in its gaseous state, had a unique emission and absorption spectra when examined at a constant temperature. In his breakthrough, Kirchhoff paved the way for modern spectrometry. Later combined with the theory of quantum mechanics, the emission spectrum of unique elements and compounds could be explained on a fundamental level by the understanding that all spectral lines are the product of any substance's quantized energy states. Since the time of Kirchhoff, the field of spectrometry has come to include a large array of possible analytical procedures, including emission and absorption of most wavelengths of electromagnetic radiation, nuclear magnetic resonance, Mössbauer spectroscopy, anti-Stokes Raman, and Stokes Raman spectroscopy¹¹.

Raman Spectroscopy

The effect that now bears Sir C.V. Raman's name was first discovered in 1928. Raman spectroscopy is an extremely useful tool that has applications in physics, chemistry, biology and engineering. When coherent light of known energy and wavelength is shone on a material, the Raman effect describes why the energy of the omitted light is different than that of the incident light. Figure 6 illustrates the three main types of scattering. In Rayleigh scattering, photons scatter off individual particles such as atoms or molecules; the energy of the photon remains constant while the direction of it is changed drastically (Fig. 6a). In Stokes Raman scattering (the Raman effect), a photon hits a molecule and scatters with smaller energy¹³ (Fig. 6b). The remaining energy is used to set the bonds of the molecules into vibration; because the bonds of each molecule are different, the energy that goes into the vibration of the molecules is different for each molecule. Thus the change in energy between the incident photon and scattered photon

is unique for each molecule, and by using a known energy light source and a spectrometer to look at the scattered light, this change may be found and the molecule identified. This process requires the bonds of the molecule have some freedom to vibrate in order to create a change in energy. As shown in Equation 3, the energy of vibration emitted from the source can be calculated by subtracting the inverse of the emitted wavelength from the inverse of the original wavelength of the laser:

$$\frac{1}{\lambda_{laser}} - \frac{1}{\lambda_{emitted}} = E_{vib} \quad (3)$$

A variant of this process is Anti-Stokes scattering. This process is identical to Raman spectroscopy except the molecule is already vibrating, commonly because of thermal energy, and as a result the photon scatters with more energy than it begins with¹³ (Fig. 6c). This effect becomes stronger as the temperature of the molecule increases, but it is almost always weaker than Stokes scattering, and comparison between Stokes and Anti-Stokes scattering can even be used to calculate the temperature of the molecule. Our experiment focused on Stokes Raman scattering and its effects.

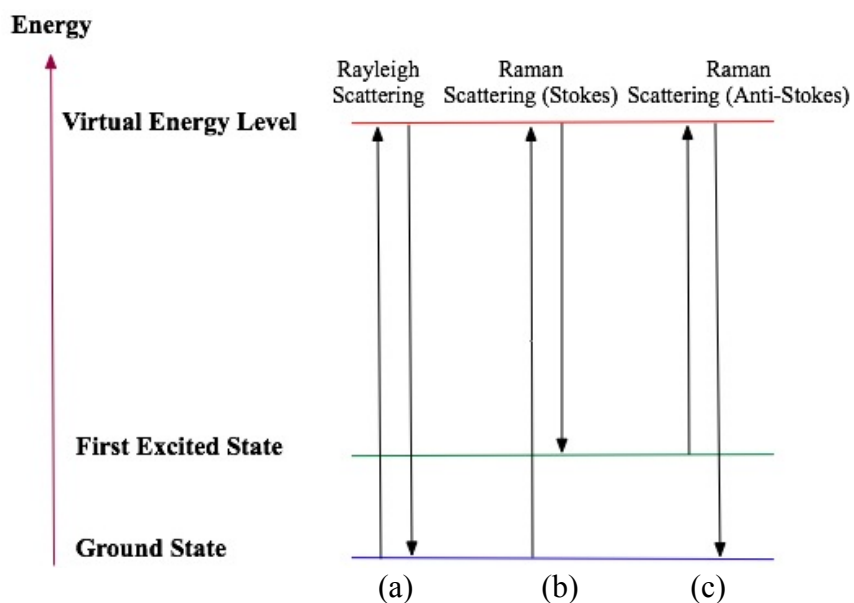


Figure 6. Types of Scattering¹⁴. (a) Rayleigh Scattering, where a photon hits a molecule and changes direction while energy remains constant, (b) Stokes Raman scattering, where a photon hits a molecule and loses some of its energy to molecular vibrations, and (c) Anti-Stokes Raman scattering, where a photon hits an already vibrating molecule and gains energy from the molecular vibrations.

In Raman spectroscopy, the energy difference between the incident and scattered photons is called the Raman shift. Even though the scattered photon has less energy, the Raman shift is, by convention, positive. The spectrum that is seen when the light scattered off the material is put through a spectrometer is called the Raman spectrum. A typical unfiltered Raman spectrum consists of the large peak at the wavelength of the laser light, surrounded by smaller satellite peaks. The Raman effect creates these satellite peaks, but because the Raman effect is rather weak these peaks are only a small fraction (less than 10%) of the energy in the laser. Due to

these peaks being rather weak, any fluorescence or stray light can interfere with and overwhelm the Raman spectrum¹³.

Applications of Raman Spectroscopy

As previously described, by comparing Stokes and Anti-Stokes scattering, Raman spectroscopy can be used to find the temperature of molecules. It can also be used to find the orientation and structure of crystals in a sample. Radial breathing, the vibration of some organic molecules arranged in loops as they grow and wane in diameter, can be used to measure the diameter of carbon nanotubes¹⁵. A special kind of Raman spectrum, called spatially-offset Raman spectroscopy, is useful for performing chemical analysis of materials beneath surfaces. This technology also has applications in the medical field, where it can unobtrusively measure the composition of materials inside the body and verify the composition of pharmaceuticals without opening their packaging¹⁶. Raman Spectroscopy also has applications in security where it is used to find hidden explosives and contraband. Environmentally, Raman spectroscopy is used to identify water pollutants and deliver real time analysis of the contaminants in water¹⁷. Moreover, Raman spectroscopy is applied in oenology to identify the levels of different substances in wine through its opaque glass, including the level of alcohol. This allows winemakers to test the quality and taste of their wine in the bottle, and identify changes from year to year¹⁸. Because of its extremely mild effects on analyzed material, Raman spectroscopy is used by art historians and conservators to analyze the composition of a particular work of art without damaging or altering the piece¹⁹. Additionally, Raman spectroscopy is used to check quality in electronics, especially when studying semiconductors, as it is important to measure the stress and temperature of a material²⁰.

EXPERIMENTAL DESIGN/APPARATUS

First Setup: HeNe Laser

The Raman Spectrometer used in this study (Fig. 7) was constructed from relatively inexpensive commercial components. A Melles Griot 0143DY-1 15mW helium-neon laser powered by a Melles Griot 25-LHP-171-249 power supply was situated in front of a breadboard. The laser was pointed towards the flat side of a six cm focal length plano-convex lens, which concentrated the laser into a single point. At this point was placed an anti-fluorescent plastic cuvette. The cuvette was used to hold the samples that were analyzed in this study. When the laser was focused into the cuvette, part of the beam was scattered 90 degrees. Some of this scattered light consisted of light from the original laser, while other parts of the light consisted of Raman shifted light. A 1 inch aspheric plano-convex lens, with a focal length of two centimeters, was placed so that the site of scatter at the cuvette was at its focal length. The flat side of the lens was placed facing the cuvette to refract the incident light as a parallel beam. A Thorlabs FMP1 long-pass wavelength filter was placed after the lens to block all wavelengths of light under 650nm, disallowing the laser light to enter the rounded side of a second plano-convex lens of the same focal length. This lens focused the parallel beams of light back to a point, where it was intercepted by a fiber-optic cable (Ocean Optics EOS00390) connected to an Ocean Optics USB2000 spectrometer.

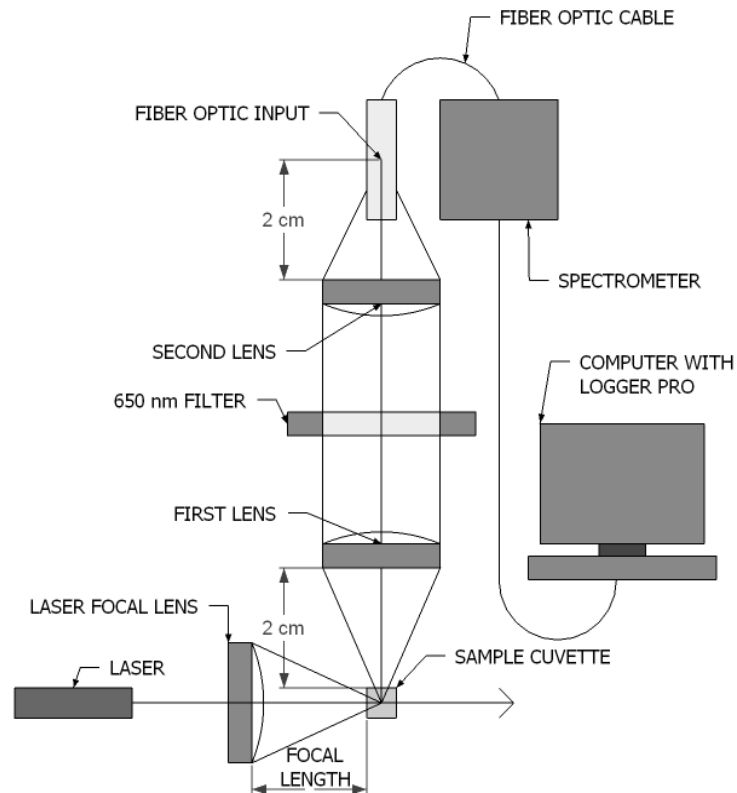


Figure 7. Initial Setup. First spectroscopy setup using the 632.8nm HeNe laser.

Once inside the spectrometer (Fig. 8), the light enters and is focused at the fiber input source. The source is located at the focus of a collimating mirror (M_1), where the incident light is reflected as parallel beams. The reflected light then hits a diffraction grating, where it is split into its component wavelengths. These components of light are then reflected by a curved mirror (M_2) onto a charge-coupled device array, which sends collected data to a computer.

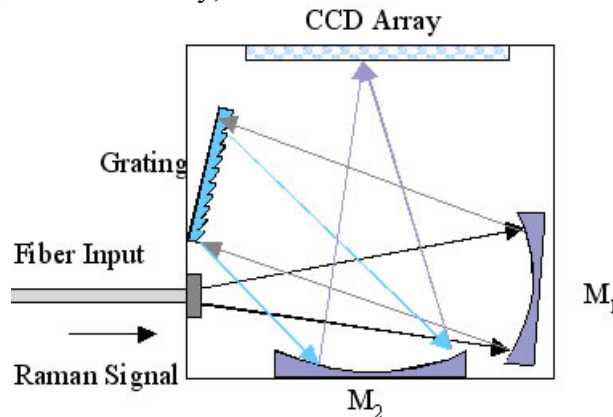


Figure 8. Spectrometer²¹. Internal structure of an Ocean Optics Spectrometer.

A computer program called Logger Pro 3.6.0 interpreted the data collected from the spectrometer.

However, when the apparatus were built, they did not initially function as expected. When first tested, they were imprecise and the data collected was not accurate. This mishap was a result of manual error and the inability of experimenters to precisely line up the lenses in their

correct focal ranges. It is difficult to position a lens exactly 2 cm away from the reflected laser light because of inaccurate equipment and the difficulty of judging off one's eye. Although the helium-neon setup was eventually calibrated successfully, a new, previously prepared setup was also used as a contingency.

Second Setup: Argon Ion Laser

The second apparatus (Fig. 9, photo in Appendix) used a 488nm Spectra-Physics 12734 25mW argon ion laser, with a Spectra-Physics 262H power supply. The laser beam was reflected off of two mirrors and through a polarizer (Thorlabs Wave Plate) in order to produce plane-polarized light. After passing through the polarizer, the laser beam was passed through a 488nm filter (Thorlabs LMR1) to eliminate all light except for the laser beam light as all other light are below 488nm. It then passed through an aperture used to narrow the beam to a smaller point, and then it passed through a lens with a 2cm focal length to focus the beam. The beam then entered a cuvette containing the samples. Similar to the previous setup, some of the beam scattered 90 degrees and entered a lens. However, the lens used this time was an aspheric collecting lens with a 2cm focus. The aspheric lens eliminated spherical aberration and helped focus the light. Next, the lens entered a long-pass wavelength filter (Thorlabs TRF90), which allows only light over 488nm to pass through. The light then passed through a second lens with a 2cm focal length in order to focus the light back to a point. Finally, the focused light entered the Ocean Optics GF081407-43 fiber optic cable leading to the Ocean Optics Red Tide USB650 spectrometer, which functions in the same manner as the spectrometer detailed in Figure 8.

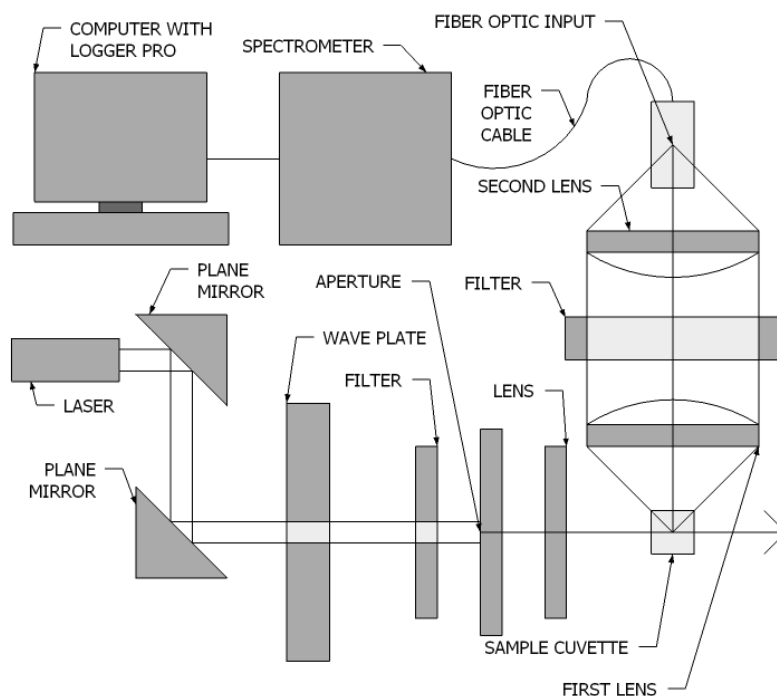


Figure 9. Advanced Setup. Second spectroscopy setup, using additional components and a 488nm argon ion laser.

When the lasers were passed through nearly identical solutions, significant differences appeared on both the Raman graph as well as the relative intensity graph. As shown in Figure 10,

the Raman peaks of methanol are much more clearly distinguishable in the argon ion setup. Additionally, there is much less noise and extraneous points.

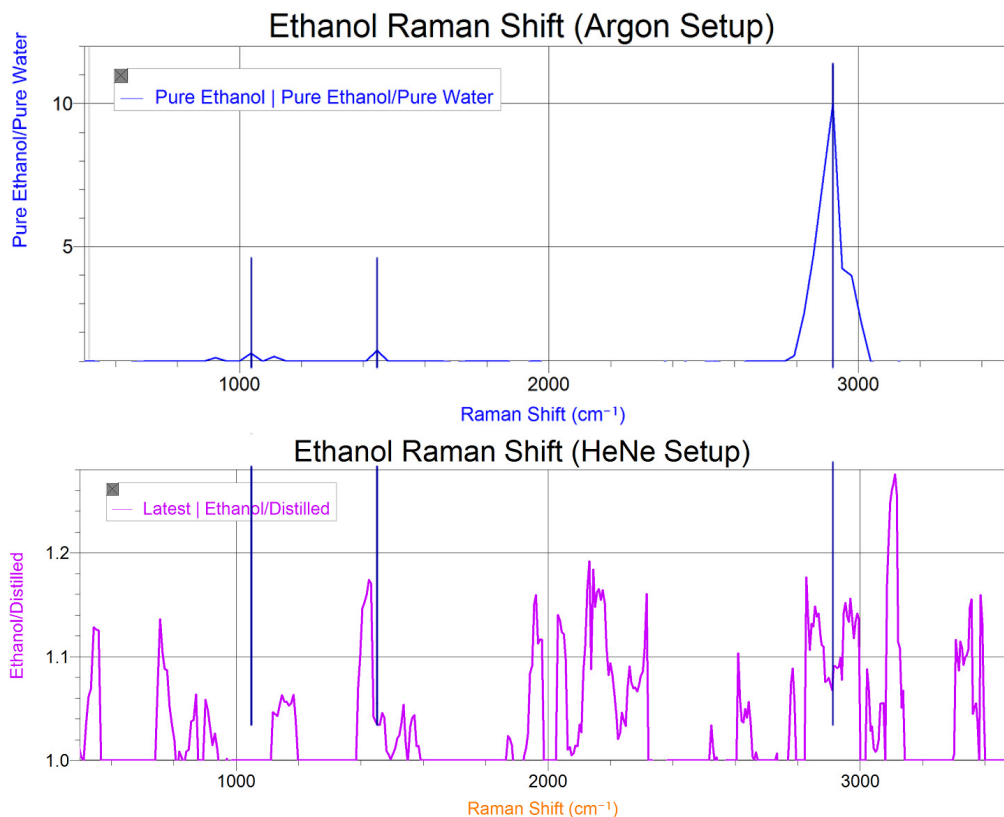


Figure 10. Comparison of Graphs of Raman Spectra Using Two Separate Apparatus. The HeNe spectrometer had a significantly higher amount of noise, especially in the 1800 cm⁻¹ to 2500 cm⁻¹ range.

DATA ANALYSIS

Determination of Ethanol and Methanol Raman Spectra

In this experiment, we tested the HeNe laser Raman spectrometer's effectiveness in identifying organic compounds. The Raman shift was recorded by first running a background reading of an empty cuvette in order to remove noise from the final reading. Next, the cuvette was filled with the organic alcohol and another Raman reading was recorded. To calculate the Raman shift, the alcohol intensity spectrum was divided by the background spectrum, yielding the Raman shift of the alcohol. Two spectra were calculated for methanol, one using the HeNe setup and one using the argon ion laser setup (Fig. 11). The Logger Pro program includes a wavelength smoothing feature, which reduces noise by averaging values into a fitted curve. Two readings were taken for ethanol at two separate wavelength smoothing values with the HeNe laser and four readings were taken at varying concentrations of Ethanol with the argon ion laser (Fig. 12).

When compared to an accepted Raman spectra reading, the HeNe readings showed considerable noise and a difference of 50 cm⁻¹ from the accepted value. In contrast, the argon ion laser spectrometer data was extremely accurate and had minimal noise, indicating a greater precision of the instruments and setup.

With the argon ion setup, we observed very accurate peaks for ethanol around 2900 cm^{-1} (Fig. 12). Upon further examination of the ethanol at various concentrations, an exponential decay graph was produced (Fig. 13); this figure demonstrates that as the concentration (molarity) decreased, it becomes more difficult to detect significant Raman lines.

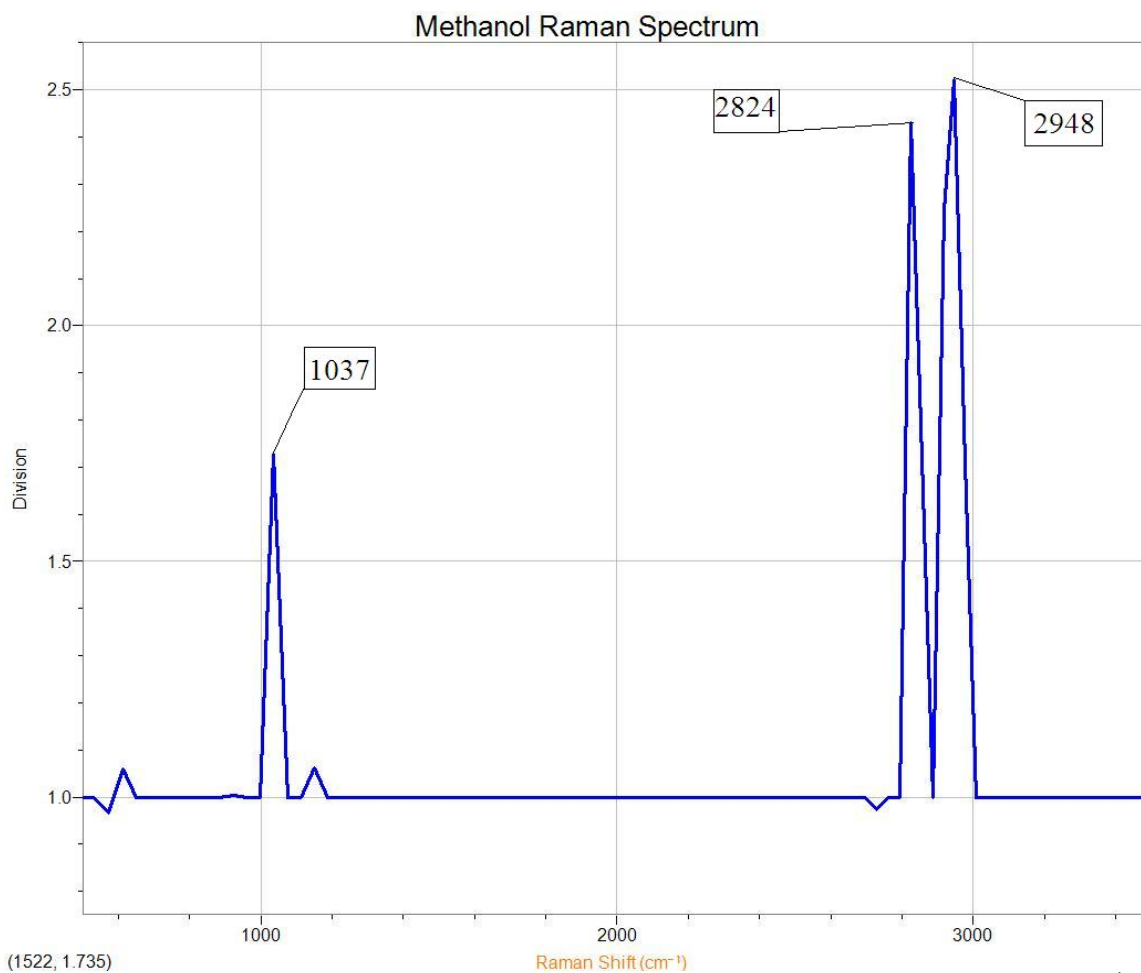


Figure 11. Methanol Raman Peaks. Raman peaks for methanol occur at 1037, 2824, and 2948 cm^{-1} using the argon ion laser setup.

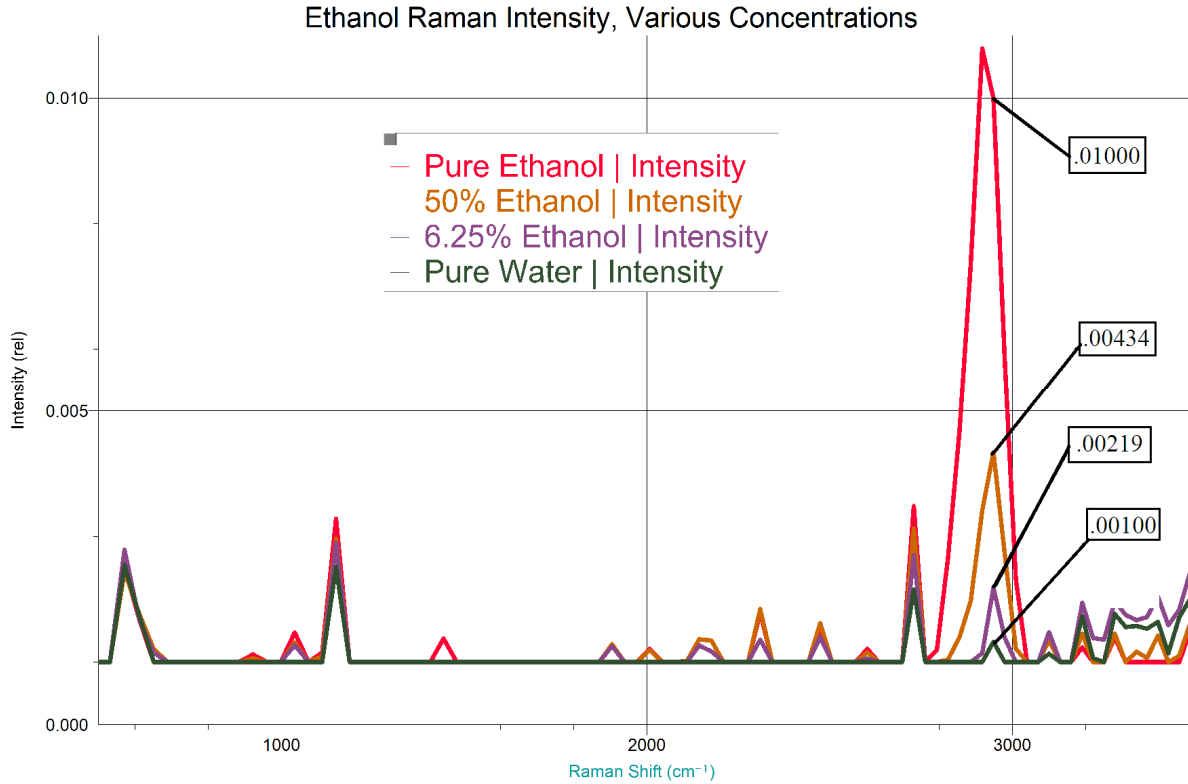


Figure 12. Raman Lines for Ethanol at Various Concentrations. A depiction of the different peaks ethanol displays at distinct concentrations. The area of most interest is where the large spike occurs around 3000 cm^{-1} . The pink line shows the Raman shift for 100% pure ethanol, the tan line shows 50% ethanol, the purple line shows 6.25% ethanol, and the dark green line is the baseline measure, showing pure water.

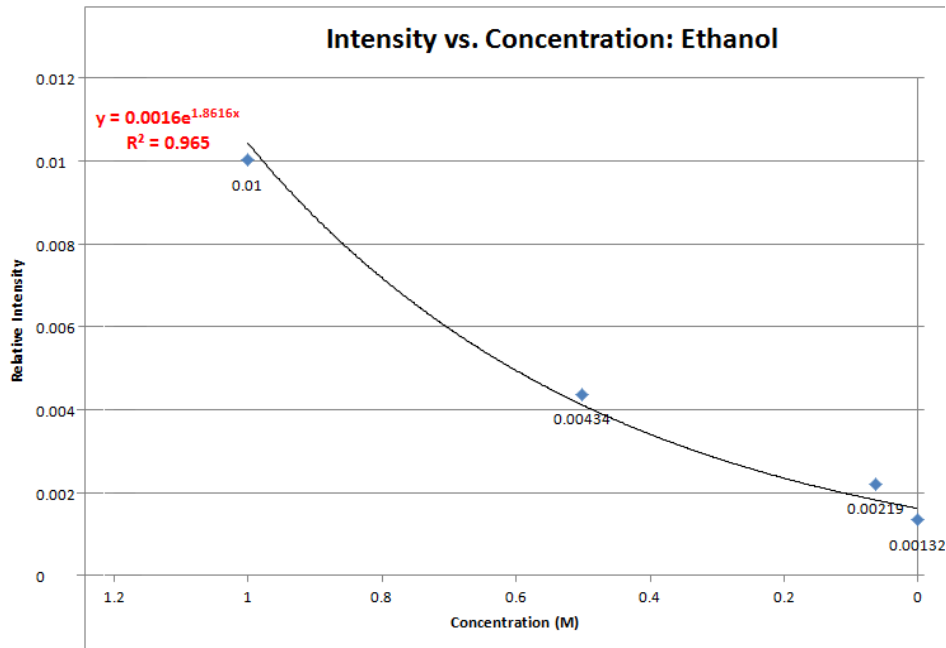


Figure 13. Relative Intensity Compared to Different Concentrations of Ethanol. A graph of the intensity of different peak concentrations of ethanol from Figure 12. The graph shows that as the concentration decreases, the intensity of the peaks also decreases, making the Raman shifts harder to detect.

Analysis of Drinking Water Sources

A number of samples--fountain water, Glaceau SmartWater (a brand of bottled water), and distilled water--were taken from different local and commercial drinking water sources and analyzed by the argon ion laser's as well as the HeNe laser's Raman spectrometer. The procedure for testing these samples resembled the procedure we used to test the organic compounds, except that distilled water was used in place of an empty cuvette as a background reading. Based on data from the HeNe laser, none of the samples' Raman spectra showed large variations from those of distilled water (Fig. 14a). However, the method of dividing the sample spectrum by the background spectra did yield some signs of Raman shift, although it is unclear if these slight shifts were the result of a difference in composition or just the product of random noise. If there is a common chemical composition between all four different samples and distilled water, it exists in a concentration too low to show clearly on the HeNe Raman spectrometer setup.

The same test was performed with the argon ion spectrometer, and as a result of the higher accuracy of the setup fountain water showed significant deviations from distilled water. This phenomenon is evident in Figure 14b by numerous large Raman shift peaks and a clear difference between distilled water intensity and fountain water intensity. This data suggests that there exists a number of additives in fountain water that are absent from distilled water.

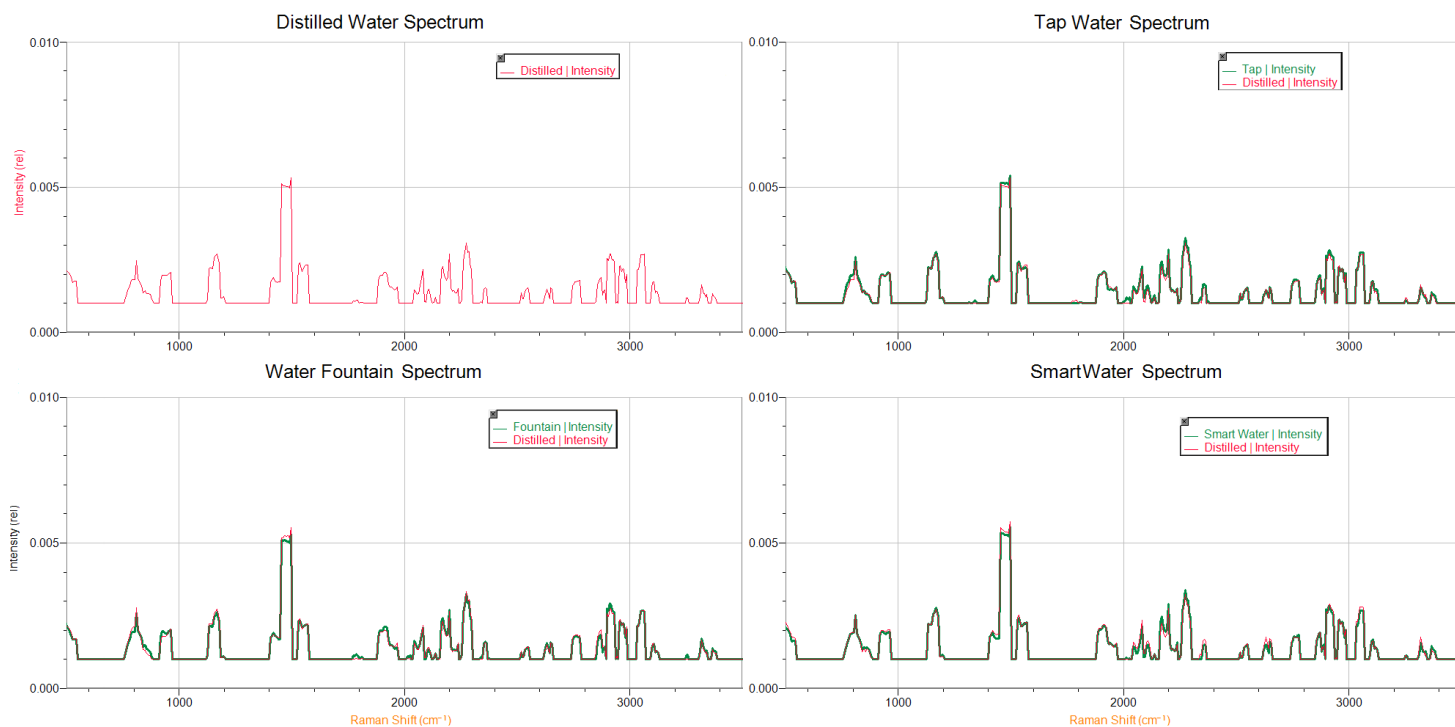


Figure 14a. Comparison of distilled water Raman intensities to tap water, water fountain, and SmartWater samples taken with the HeNe laser spectrometer.

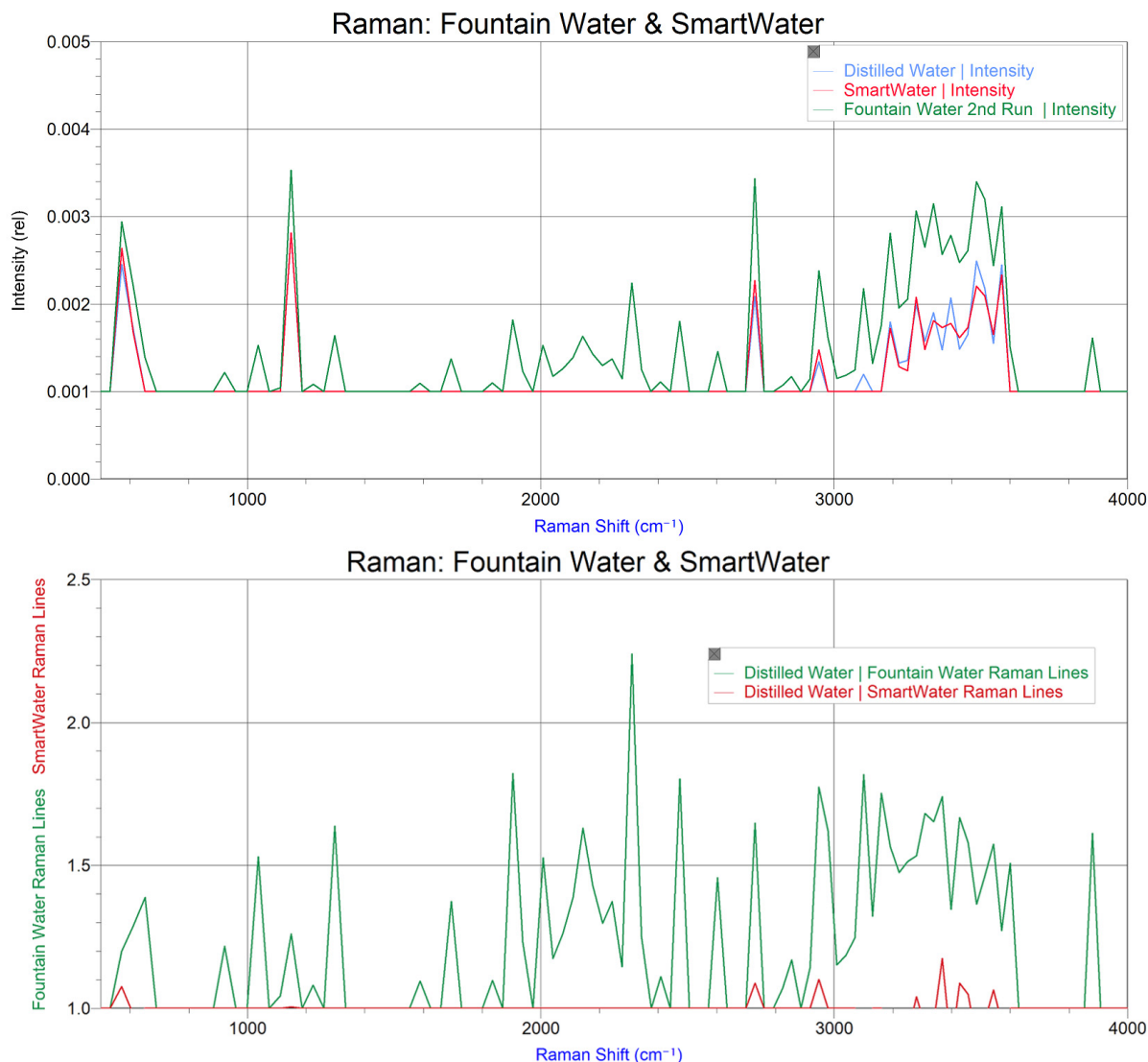


Figure 14b. Raman Shifts for Two Water Samples. For the top image, the Raman shift for fountain water is the green line on top and the Raman shift for Smart Water is the red line at the bottom. It can be seen that there is a significant difference in the contents of the two waters (the large mountain-shaped peak represents foreign molecules). For the bottom image, fountain water's intensity is the green line on top, SmartWater's intensity is the red line beneath it, and distilled water's intensity (control) is the blue line on the bottom. The bottom graph shows the relative intensity of the three water samples, as opposed to the top graph, which shows the divided comparison (Raman shift). The bottom graph more accurately shows how fountain water shows significant Raman peaks, as deviations from distilled water occur around 2000 cm^{-1} and 3400 cm^{-1} .

Analysis of Fertilizer Samples of Varying Concentration

Using the argon ion laser setup, we analyzed different concentrations of fertilizer solution. The Raman spectra of distilled water was taken and used as the baseline reading (the control). The first sample analyzed was a saturated solution of Schultz-Instant fertilizer, with 6 grams of fertilizer dissolved in 12.2 mL of distilled water, the maximum concentration of

fertilizer we tested. After dividing the intensity of the saturated fertilizer solution by the intensity of the distilled water (the baseline), we found that the Raman shifts for fertilizer were large, numerous, and frequent. The run yielded the expected results as fertilizer contains many complex compounds such as nitrates, phosphates, and other organic materials. After testing the saturated solution of fertilizer, the concentrations of subsequent samples were quartered: the second sample was 25% saturated, with 1.5 grams of fertilizer in 12.2 mL distilled water, the third sample was 6.25% saturated, with 0.375 grams of fertilizer in 12.2 mL distilled water, and the fourth sample was 1.5625% saturated, with .09375 grams of fertilizer in 12.2 mL distilled water. We found that as the concentration of fertilizer decreased, the intensity (height) of the Raman peaks decreased, and the fertilizer spectra approached (but never matched) the distilled water spectrum (Fig. 15). We were also able to compare our data to definitive Raman peaks found on the Internet, which allowed us to identify phosphates and nitrates present in the fertilizer.

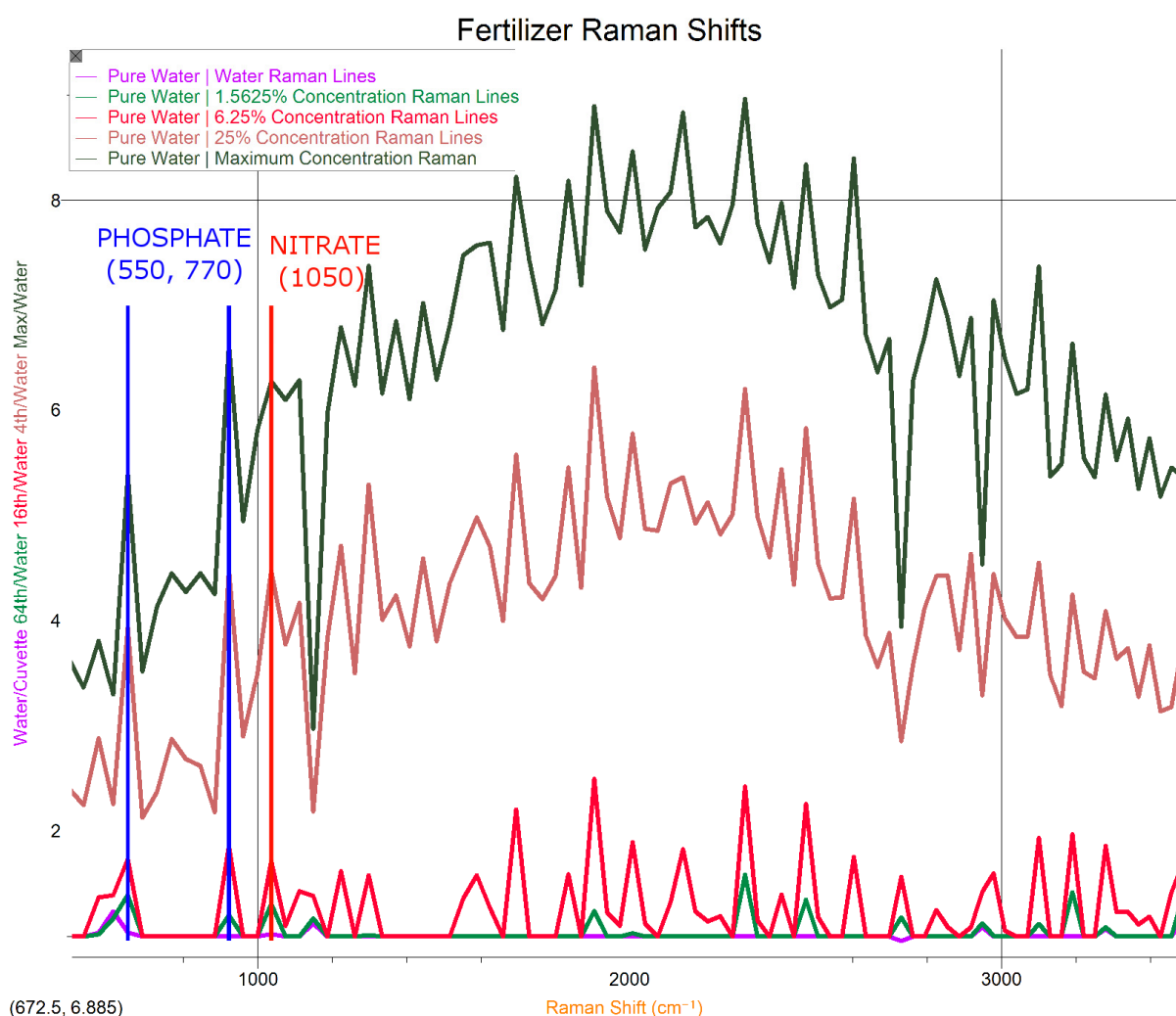


Figure 15. Raman Lines for Different Concentrations of Fertilizer. The large number of peaks in the Raman spectrum of fertilizer can be attributed to the complex chemical composition of fertilizer. Highlighted in red is the primary nitrate Raman peak and in green are the two phosphate Raman peaks. As the concentration of fertilizer decreases, the intensity of the peaks decreases, and the spectrum approaches that of distilled water. Particularly of note are the Raman peaks at 550 cm⁻¹, 770 cm⁻¹ and 1050 cm⁻¹, which correspond to chemicals containing phosphates and nitrate, respectively.

Accepted values of 550 cm^{-1} , 770 cm^{-1} and 1050 cm^{-1} for both phosphate and nitrogen Raman shifts were used to analyze the fertilizer spectrum. There were sharp peaks in the fertilizer's Raman shift which corresponded to the accepted peaks for phosphate and nitrogen, thus showing the presence of these molecules in the fertilizer samples.

Analysis of Pollutants in a Freshwater Ecosystem

The greatest impact fertilizer run-off has on a freshwater ecosystem is its release of nitrate and phosphate molecules. These ions, in high concentrations, increase the primary productivity of the ecosystem and allow algae and other aquatic plants to flourish. This phenomenon, known as eutrophication, ultimately reduces the amount of oxygen in the water, soon displacing or killing other organisms that are necessary for the freshwater ecosystem to function properly. The fertilizer run-off that causes these algal blooms has several detrimental effects on the freshwater ecosystem.

Both the HeNe and Argon laser spectrometers were used to investigate the effects of fertilizer on a freshwater body's nitrate and phosphate concentrations. In the previous experiment, the Argon laser was utilized to determine the Raman spectrum for varying concentrations of commercial fertilizer. Next, a sample of pond water was taken from a freshwater pond on the Drew University campus and then analyzed by the HeNe spectrometer. The data collected showed large peaks in the 350 cm^{-1} to 1500 cm^{-1} range, and a number of smaller, more scattered peaks from 1750 cm^{-1} to 2500 cm^{-1} . The high intensity of the 350 cm^{-1} to 1500 cm^{-1} range peaks can be explained by the high amount of biological matter present in a freshwater pond, in the form of living molecules and detritus (dead organic matter). Figure 16 displays normalized amplitudes for both our experimental pond sample spectrum and an empirical fertilizer spectrum with isolated nitrate and phosphate peaks.

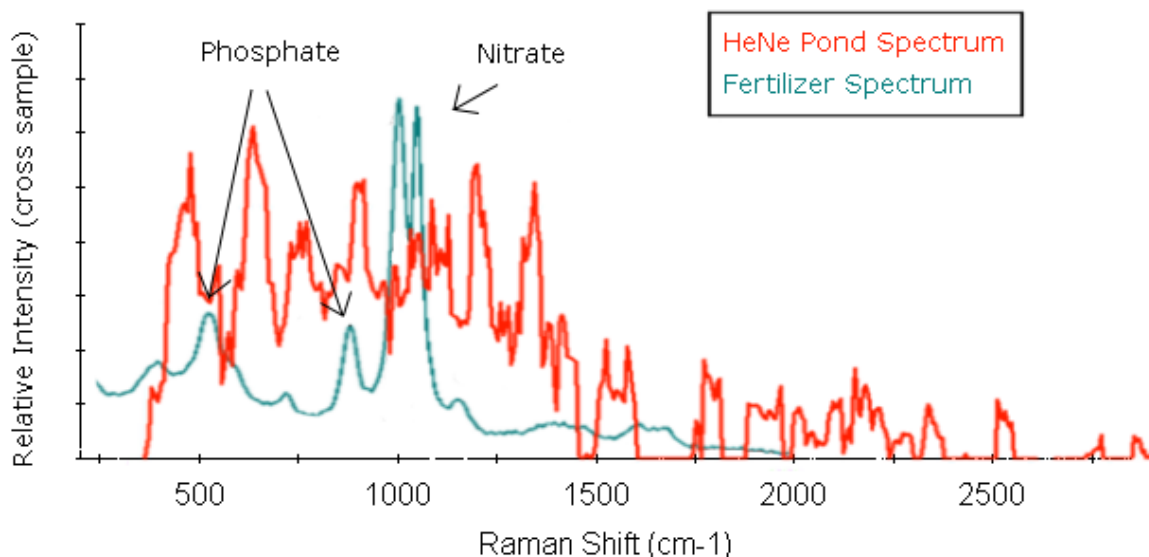


Figure 16. Pond Water and Fertilizer²². Comparison of the HeNe pond sample spectrum to an accepted fertilizer spectrum. The phosphate peaks occur at 550 cm^{-1} and 770 cm^{-1} , while the nitrate peak occurs at 1050 cm^{-1} .

Despite the considerable noise possibly caused by present organic molecules, Raman spectroscopy proved effective enough to show the presence of fertilizer pollutants in the sample. The peaks of phosphate and nitrate (550 , 770 cm^{-1} and 1050 cm^{-1} respectively) lie within the range of the high Raman shift due to organic matter in the pond sample. However, they are still noticeable to some degree. The secondary peak of phosphate (770 cm^{-1}) was noticeable in the pond sample at 775 cm^{-1} , which is well within the HeNe spectrometer's margin of error as evident by the previous alcohol based calibration experiments. To a lesser extent, the primary phosphate peak and nitrate peaks can be seen within the pond sample spectrum, but due to organic noise they are less clear than the 770 cm^{-1} peak.

CONCLUSION

Determination of Ethanol and Methanol Raman Spectra

The accuracy of the constructed HeNe laser was compared to that of the pre-assembled Argon laser. Discrepancy between the spectra readings of two organic alcohols, methanol and ethanol, showed great difference between the accuracy of the two spectrometers (Fig. 10); the argon ion laser setup was clearly more precise in minimizing noise and pronouncing peaks. After determining that the Argon spectrometer had greater sensitivity to the Raman shift, it was further used to investigate the effects of concentration on Raman shift. By repeating the procedure for several samples of ethanol of varying concentration, we confirmed a direct relationship between concentration and Raman shift intensity: as the concentration of a particular sample decreases, Raman shift of the sample becomes more difficult to detect.

Analysis of Drinking Water Sources

The drinking water spectra showed that commercial bottled water and tap water contain no significant differences from distilled water. The HeNe spectrometer showed that all samples were very similar in content, which is to be expected in any collection of safe drinking water. However, the greater accuracy of the Argon spectrometer allowed the small differences between fountain water and distilled water to be measured.

In follow up experiments, more spectroscopic data could be collected to match each Raman line with a unique vibrational energy value, signaling different bond lengths and attractions. For example, through further analysis of Figures 11 and 12, one may determine certain Raman peaks to be C-H or O-H bonds. This information could then be pieced together to determine the identity of potentially organic and/or malicious molecules. The data represented in Figure 11 would also support SmartWater's claim to contain 100% vapor distilled water, as dividing SmartWater's intensity by distilled water's intensity produced very few Raman peaks; the two sources of water have very similar composition. The minor Raman peaks in the 3200 - 3600 cm^{-1} can perhaps be explained by the inclusion of electrolytes, a component of SmartWater that is obviously not present in distilled or deionized water.

Analysis of Fertilizer Samples of Varying Concentration

The argon ion laser spectrometer showed that fertilizer was detectable even at $1/64^{\text{th}}$ concentration. This data leads to the conclusion that the chemical components which make up Schultz-Instant fertilizer will also be detectable at this severely diluted concentration. Thus,

phosphate and nitrate, two molecules present in commercial fertilizer, are detectable at low concentration in water. This data suggests Raman spectroscopy may have further application in agricultural sciences and biology.

Analysis of Pollutants in a Freshwater Ecosystem

The two pollutants which led to algal bloom, phosphate and nitrogen, could be seen to a moderate extent in a sample of local pond water. However, because there was no control sample in this study, due to availability and time constraints, not many concrete conclusions can be made about the environmental state of this sampled pond. If a control sample was taken, perhaps from a wildlife reserve, and used as a background spectrum the pollution in another sample could be better measured.

REFERENCES

1. Abramowitz M, Fellers TJ, Davidson MW. The Nature of Electromagnetic Radiation [Internet]. Olympus America Inc; 2010 [cited 2010 Jul 28]. Available from: <http://www.olympusmicro.com/primer/lightandcolor/electromagintro.html>
2. Colwell CH, compiler. PhysicsLAB: Converging Lenses [Internet]. 2010 [cited 2010 Jul 28]. Available from: http://dev.physicslab.org/Document.aspx?doctype=3&filename=GeometricOptics_ConvergingLenses.xml
3. Nave CR, compiler. Spherical Aberration [Internet]. Atlanta (GA): HyperPhysics by Georgia State University Department of Physics and Astronomy; 2005 [cited 2010 Jul 29]. Available from: <http://hyperphysics.phy-astr.gsu.edu/hbase/geoopt/aber.html>
4. Pollock S. Lab 4. Lenses [Internet]. 2010 [cited 2010 Jul 28]. Figure 2. Lens. Available from: http://www.colorado.edu/physics/phys2020/phys2020_fa01/labs/lab4mod.htm
5. Ullrich B. Introduction in Optics II [Internet]. 2008 [cited 2010 Jul 28]. Figure 1. Converging lens. Available from: <http://kottan-labs.bgsu.edu/teaching/workshop2001/chapter2.htm>
6. Patterson B, Quealy E, compilers. 2000. How Fiber Optic Cabling Works [Internet]. Ames (IA): Iowa State University Department of Computer Science. [cited 27 Jul 2010]. Available from: <http://www.cs.iastate.edu/~patterbj/cs/FiberWWW/how.htm>
7. Crowell B. Optics: Refraction [Internet]. 2010 [cited 2010 Jul 28]. Figure K. Total internal reflection in a fiber-optic cable. Available from: http://www.lightandmatter.com/html_books/5op/ch04/ch04.html
8. Nave CR, compiler. Gas Lasers [Internet]. Atlanta, GA: HyperPhysics by Georgia State University Department of Physics and Astronomy; 2005 [cited 2010 Jul 28]. Available from: <http://hyperphysics.phy-astr.gsu.edu/hbase/optmod/lasgas.html>
9. Goldwasser SM. Helium-Neon Lasers [Internet]. 2010 [cited 2010 Jul 28]. Typical HeNe Laser Tube Structure and Connections. Available from: <http://www.k3pgp.org/Notebook/Lasersam/laserhen.htm#henhlc0>
10. Beach N. The Argon Ion Laser [Internet]. Gainesville, Florida: University of Florida ITL; 1996 [cited 2010 Jul 28]. Available from: http://itl.chem.ufl.edu/4411L_f96/i2_lif/ar_laser.html
11. MIT Spectroscopy Lab. The Era of Classical Spectroscopy [Internet]. [Updated 2010 Jan 12]. Cambridge (MA): Massachusetts Institute of Technology, MIT Spectroscopy. [cited 2010 Jul 25]. Available from: <http://web.mit.edu/spectroscopy/history/history-classical.html>

12. Wade A. Color Facts and Color Theories [Internet]. 2010 [cited 2010 Jul 28]. Figure 1. Diagram of Isaac Newton's experiment that shows how a beam of white light, passed through a prism, is refracted and broken up into the colors of the spectrum. Available from: <http://www.paintcolorchart.net/paintcolorchart02.php>
13. Somerville WRC, Le Ru EC, Northcote PT, Etchegoin PG. 2010. High performance Raman spectroscopy with simple optical components. Am J Phys [Internet]. [cited 2010 Jul 26]; 78(7): 671-677. Available from: <http://scitation.aip.org/getpdf/servlet/GetPDFServlet?filetype=pdf&id=AJPIAS00007800007000671000001&idtype=cvips&prog=normal>
14. Alexander K. State of the Art Surface-Enhanced Raman Spectroscopy: Searching for the Perfect SERS Substrate [Internet]. 2008 [cited 2010 Jul 28]. Figure 1. A schematic illustration of the differences between Rayleigh (elastic) and Raman (inelastic) scattering. [about 1 screen]. Available from: <http://www.physics.unc.edu/project/rln/kristen/>
15. Dresselhaus MS, Dresselhaus G, Saito R, Jorio A. 2004. Raman spectroscopy of carbon nanotubes. Physics Reports [Internet]. [cited 2010 Jul 27]; 409(2): 27-46. Available from: <http://mgm.mit.edu/papers/i1049.pdf>
16. Spatially Offset Raman Spectroscopy (SORS) [Internet]. Oxfordshire, UK: Cobalt Light Systems Ltd.; 2010 [cited 2010 Jul 28]. Available from: <http://www.coballight.com/technology/spatially-offset-raman-spectroscopy>
17. OptoIQ. 2004. SERS traces water pollution in real time [Internet]. Laser Focus World. [cited 2010 Jul 25]. Available from: <http://www.optoiq.com/index/photronics-technologies-applications/lfw-display/lfw-article-display/206869/articles/laser-focus-world/volume-40/issue-6/world-news/world-news/sers-traces-water-pollution-in-real-time.html>
18. Alexander R. 2008. Advantages of Raman Spectroscopy when Analyzing Materials Through Glass or Polymer Containers and in Aqueous Solution [Internet]. Waltham (MA): PerkinElmer, Inc. [cited 2010 Jul 26]; 6 p. Available from: http://las.perkinelmer.com/content/applicationnotes/app_ramananalysissthroughglasspolymeraqueous.pdf
19. Art and Heritage [Internet]. Hoffman Estates, IL: Renishaw plc; 2010 [cited 2010 Jul 28]. Available from: <http://www.renishaw.com/en/art-and-heritage--7982>
20. Semiconductors [Internet]. Hoffman Estates, IL: Renishaw plc; 2010 [cited 2010 Jul 28]. Available from: <http://www.renishaw.com/en/semiconductors--7983>
21. Chen G, Kang JU. Photonics and Optoelectronics Lab: Raman spectroscopy based on frequency doubled Yb-doped fiber laser [Internet]. Baltimore, MD: Johns Hopkins University Electrical and Computer Engineering; 2007 [cited 2010 Jul 28]. Available from: <http://www.ece.jhu.edu/photronics/research/research07.htm>
22. Nazarenko A. Quantitative Measurements of Inorganic Anions in Solutions [Internet]. Buffalo, New York: Buffalo State College Department of Chemistry; 2006 [cited 2010 Jul 28]. Available from: <http://staff.buffalostate.edu/nazareay/jcej/3.htm>

APPENDIX

The following image shows the first spectroscopy apparatus used in this study, which was implemented using a helium-neon laser. However, due to calibration issues, a second apparatus was also used.



The following image shows the second spectroscopy apparatus used, implemented with an argon-ion laser.

